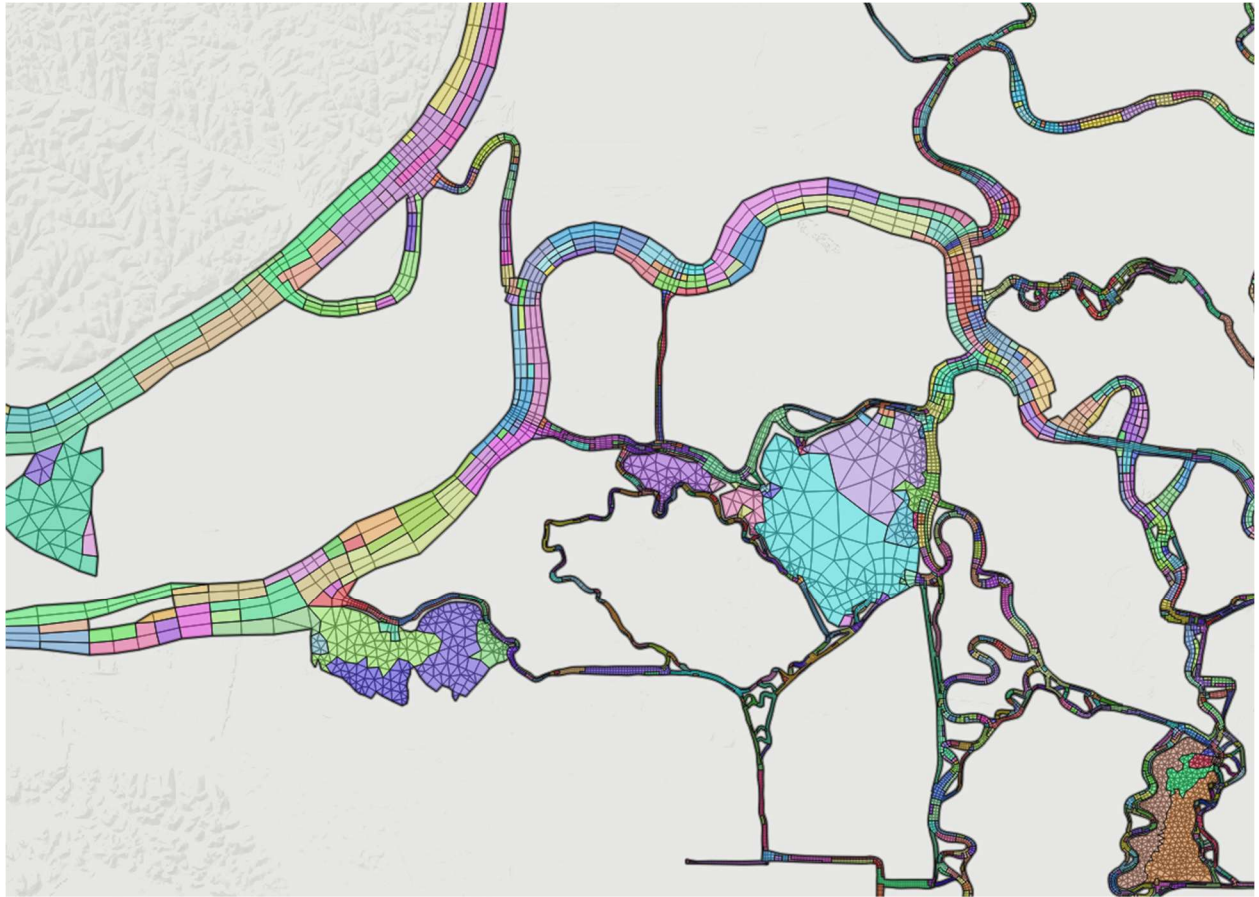


Delta-Suisun Biogeochemical Model Development: Year 2 Progress



By Zhenlin Zhang, David Senn and Alexandra King

SFEI Contribution #961



Executive Summary

To address the complex and multi-purpose management needs for the Sacramento-San Joaquin Delta and Suisun Bay, we present a three-dimensional, mechanistic biogeochemical cycling model that includes nitrogen transformation, phytoplankton dynamics, grazing by zooplankton and clams, and detrital organic processes. Such a mechanistic model provides a holistic approach to quantify the intricate interactions and dependency among the key model variables and can be used as a powerful tool to evaluate the system response to management actions and environmental conditions. To significantly reduce model computational time, an attribute-dependent model aggregation scheme based on an ArcGIS regionalization method was developed. A comparison of model results between the high-resolution model (70 000 cells) and an aggregated model (5000 cells) for nitrogen cycling shows that the aggregated model performed reasonably well in capturing the spatial and temporal variability of nitrate and ammonia and only took about 7% of the time needed for the full-resolution run. Using the aggregated grid, we further included all other biogeochemical processes and performed subsequent model tuning. Using the tuned coefficients from the aggregated model, our most recent high-resolution model shows that the modeled chlorophyll-a, nitrate and ammonia match reasonably well with the observed spatial and temporal variability in these variables. Bivalves (both *Potamocorbula* and *Corbicula*) played a central role in controlling phytoplankton biomass year round. However, due to the slow response of bivalves in growth to food availability, they may not prevent large scale blooms from happening when other conditions (such as light availability) support them. The observed level of phytoplankton biomass alone as a food source cannot fully support the observed growth in the bivalves. It is strongly suggested that other food sources, such as detritus (particulate organic matters) may be important in supplementing the food web in the ecosystem.

Contents

| | |
|--|-----------|
| Executive Summary | I |
| 1. Introduction..... | 1 |
| 2. Background..... | 1 |
| 3. Objective | 4 |
| 4. Methods..... | 5 |
| 4.1 Biogeochemical model structure..... | 5 |
| <i>4.1.1 Nutrient cycling.....</i> | <i>6</i> |
| <i>4.1.2 Phytoplankton dynamics.....</i> | <i>7</i> |
| <i>4.1.3 The Dynamic Energy Budget (DEB) Model for Clams.....</i> | <i>8</i> |
| <i>4.1.4 The Sediment Diagenesis Model</i> | <i>10</i> |
| 4.2 Attribute-dependent model aggregation..... | 10 |
| 4.3 Tuning the Dynamic Energy Budget (DEB) model for benthic grazers | 13 |
| 5. Results and Discussion | 16 |
| 6. Future Work:..... | 20 |
| References..... | 21 |
| Appendix A The comparison between modeled vs. observed chlorophyll-a, NO ₃ and NH ₄ at multiple locations across the Delta and Suisun bay..... | 24 |
| Appendix B Comparisons between modeled clam grazing rate and calculated maximum grazing rate for multiple locations across the Delta and Suisun Bay. | 30 |

Figures

| | |
|--|----|
| Figure 1 The biogeochemical model structure implemented in DELWAQ | 6 |
| Figure 2 A schematic diagram of the DEB model illustrating how energy generated from food intake is distributed among different compartments of a living organism. The compartments in the black boxes (E, V, and R) are model variables for the DEB model. | 8 |
| Figure 3 The aggregated grid. Each distinct color represents a different cluster of grids for the aggregated grid..... | 12 |
| Figure 4 A comparison of modeled NH ₄ (top) and NO ₃ (bottom) between the aggregated model (left) and full resolution model (middle), and the difference between the two (right). | 13 |
| Figure 5 The initial AFDW biomass for Corbicula and Potamocorbu. | 16 |
| Figure 6 Comparisons of model results between scenarios with clams (default) and without clams (no clams)..... | 19 |
| Figure 7 Comparisons of model results between the default run and the scenario run with increased growth rate for a deep (USGS 649 on the left) and a shallow location (D7 on the right). | 20 |

Tables

| | |
|--|----|
| Table 1 The spatially and temporally averaged condition for both bivalves during the simulation period (WY2011)..... | 14 |
| Table 2 The derived rates table from the 0D DEB model satisfying the objective and constraints for model tuning..... | 14 |

1. Introduction

The Sacramento-San Joaquin River Delta and Suisun Bay system supports multiple important water usage and ecosystem functions. To provide scientific support to meet the nutrient management needs of regulators, stakeholders, and the scientific community, we need to investigate nutrient-related questions such as the source, present and future levels, spatial variability, interaction with phytoplankton and higher trophic levels, drivers and forcings, water quality impact, response to climate changes, and response to management actions. Due to the intricate inter-dependency of biogeochemical processes, the numerous spatiotemporally-varying environmental factors and the multi-purpose management challenges for the system, a process-based, quantitative, and holistic approach is essentially required to assess the nutrient impact and trend for the estuarine-riverine system and to evaluate the impact of management actions to support science-based decision making.

From 2017, we started to develop and apply a three-dimensional biogeochemical model for Sacramento-San Joaquin River Delta and Suisun bay. During the first stage of model development, we have modeled nitrification and denitrification processes, validated the model against the observed dissolved nitrate and ammonia, and developed proof-of-concept approaches to address management questions. This report describes progresses during the second-phase of model development and is outlined as follows:

- Background – Section 2
- Objectives – Section 3
- Methods – Section 4
- Results and Discussion – Section 5
- Future work – Section 6

2. Background

Nutrients and phytoplankton undergo complex biogeochemical transformations (*SFEI*, 2014) as they are transported, mixed, and dispersed through the Delta and Suisun Bay. The rates of these transformations can be strongly influenced by physical, hydrological, atmospheric and biological conditions, such as bathymetry, river discharge, light availability, winds, tides, surface

waves, turbidity, water temperature, salinity, primary production and higher trophic levels, which can all vary greatly in space and time. Thus, nutrient concentrations, including relative abundance of different forms (e.g., ammonium vs. nitrate), and indicators of response (e.g., phytoplankton biomass) exhibit strong spatial, seasonal, and inter-annual variability (e.g., *Jassby, 2008; SFEI, 2015*). In addition, major changes in some important forcings have occurred in the Delta and Suisun Bay over the past ~40 years, resulting in sudden shifts or gradual changes in the balance among ecosystem processes. The invasion of *Potamocorbula amurensis* around 1987 resulted in an abrupt drop in phytoplankton production and biomass in Suisun Bay and the western Delta (*Cloern and Jassby, 2012; Cloern, 2018; Jassby, 2008*). In addition, there is anecdotal evidence that abundances of *Potamocorbula* (the salty-region invasive clam) decreased substantially in Suisun after WY2017's extremely wet winter and spring, which could again alter the balance of important processes. Recent analyses (*Cloern and Jassby, 2012; Schoellhamer, 2011*) found that suspended sediment concentrations in Suisun Bay have decreased by ~50% since 1975, meaning that light levels available to support phytoplankton growth have essentially doubled. In addition, Regional San's 2010 National Pollution Discharge Elimination System (NPDES) permit sets May 2021 as the operational date for an upgrade to an ammonia limit of 1.7 mg-N/L (April-October) and 3 mg-N/L (November-March), and sets an interim ammonia limit of 47 mg-N/L year-round prior to the completion of the upgrade (*NPDES Permit, 2010*). Relative to the typical performance of the current treatment plant, the upgrade is anticipated to result in a >95% reduction in effluent dissolved ammonia concentration and a >65% reduction in effluent total inorganic nitrogen concentration (pers. comm., Lisa Thompson, Regional San). All these changes may influence primary production, phytoplankton biomass, and nutrient concentration in the system.

Among various biogeochemical processes, clam grazing has been hypothesized to be the cause of the observed abrupt drop in phytoplankton biomass in 1987 in the system (*Cloern, 2018; Jassby, 2008*). The presence of immobile *Potamocorbula* and *Corbicula* at the bottom imposes a 'toll' on phytoplankton biomass in the water column, which leads to a reduction of zooplankton and food supply to native fish. The grazing rate of bivalves is highly dependent on the physical, atmospheric and biological conditions of the system. Since bivalves graze at the bottom while phytoplankton typically concentrates at the surface, their grazing rate can become limited by the rate of food delivered to clams by turbulent mixing. During stratifying seasons, phytoplankton may become out of reach for the clams and thus result in starvation of clams even when primary

production and zooplankton grazing is strong. Clams generally do not respond as fast to food sources as zooplankton, so they can survive for longer period without food and are ready to take advantage of higher productivity before a bloom event. Clams can graze not only on phytoplankton, but also on detritus and zooplankton (*Crauder et al.*, 2016; *Kimmerer et al.*, 1994). Lastly, the grazing rate of clams can vary greatly in space and time; generally, small newly settled clams have much higher growth rate per biomass compared to larger mature clams.

The process-based, spatially-explicit, coupled physical-biogeochemical model has been recognized by a broader scientific and management committee as an essential tool to provide science-based decision making for nutrient management in the Delta system. In a recent “Model Steps and Scenarios” report, we detailed the role of the model in the broader context of management needs, the model steps and efforts required to develop a fully calibrated regional biogeochemical model, the model scenarios we can run to answer management questions, and how confident we are about the ability of the model to answer these questions at each model developmental stage. To make sure that the model development plan proposed is in line with the management needs of the system, we proposed five consecutive model development steps. A summary of each step is listed below.

- **Step 1** (mid-2017 to mid-2019): Customize a biogeochemical model that includes all major drivers, substances, and processes for the system for a typical non-bloom year (WY2011). The high-nutrient and low-chlorophyll condition for the chosen year is the most representative condition for the estuarine-riverine system. When this step is accomplished, we would anticipate that, to the best of our knowledge, the model has all the components needed to capture the biogeochemical processes in the system and the model should be able to produce a generally non-bloom condition in the Delta.
- **Step 2** (mid-2019 to mid-2020): In this second step of model development, we targeted at resolving drastically different modeling responses of phytoplankton dynamics during two different water years (WY2011 and WY2016): one with non-bloom and the other with bloom conditions. This would be a good starting point to assess the robustness of the model structure and parameters.
- **Step3** (mid-2020 to mid-2021): During this step, more effort will be focused on resolving the timing, amplitude, and duration of the bloom events in WY2016. We will also use the opportunity to tune rates and parameters related to dissolved oxygen (DO), where greater

fluctuations in DO are expected when system production and respiration activities are strong. We expect to obtain a set of parameters that are system-wide optimized, which will improve our confidence about the ability of the model to quantify the linkages between the drivers and modeling targets or management needs.

- **Step 4** (mid-2021 to mid-2022): At this stage of model development, the major effort will be to reconcile the spatial discrepancy between the model results and observations. Spatial variability in various environmental drivers will first be interpolated from the best-available measurement data across the Delta to each computational cell and then used to drive the model. We expect that, by improving the initial and boundary conditions of the key drivers, we will be able to improve the capability of the model to simulate the spatial variability of key modeled variables.
- **Step 5** (from mid-2022): Revise the model structure and parameters as needed and address the data gap issue.

Up until now, we are already 1.5 years into the first step and another half a year will be required to accomplish this step. In this report we will detail the substantial effort we made in developing and validating the biogeochemical model for WY2011.

3. Objective

The objective of this project is to develop and calibrate a three-dimensional finite-volume biogeochemical model (DELWAQ) offline coupled to an unstructured-grid hydrodynamic model (Dflow3D-FM) for WY 2011 in the Delta and Suisun Bay. The biogeochemical processes should include nitrogen cycling, phytoplankton dynamics, benthic and pelagic grazing, detrital organic respiration/mineralization, and a sediment diagenesis model. The model results will be calibrated against key measured variables, including nitrogen, chlorophyll-a and clam biomass across the Delta and Suisun Bay.

4. Methods

In this section, we will first demonstrate the biogeochemical model structure, the key modules we have turned on, the limitation of the chosen modeling processes, and the major uncertainties; we will then introduce a new attribute-based model aggregation method, which significantly reduces the runtime needed for the model and greatly improves the efficiency of parameter tuning; lastly, using the tuned coefficients from the aggregated model, we present comparisons between the modeling results and observations.

4.1 Biogeochemical model structure

We used a process-based, spatially-explicit, coupled hydrodynamic-biogeochemical modelling approach to model water quality in the Delta/Suisun Bay. We selected the Deltares Flexible Mesh (DFM) model and the Deltares Water Quality model (DELWAQ) as our primary platforms for coupled hydrodynamic and biogeochemical modeling for WY2011. Working in the DFM-DELWAQ platform for this project also allowed us to build upon the existing multi-year CASCaDE project¹, where extensive effort has been invested into the hydrodynamic calibration for Suisun Bay and the Delta for WY2011 and WY2012. Going forward, it is possible to take advantage of other existing hydrodynamic models in the system and couple them offline with DELWAQ, but substantial effort in developing a connector from other modeling platforms to

¹ USGS-led project, partially funded by the Delta Science Program. Collaborators: Deltares, UNESCO-IHE, and SFEI.

DELWAQ will be required. The model structure for the full biogeochemical cycling process is illustrated in the following diagram (Figure 1) and explained in detail below.

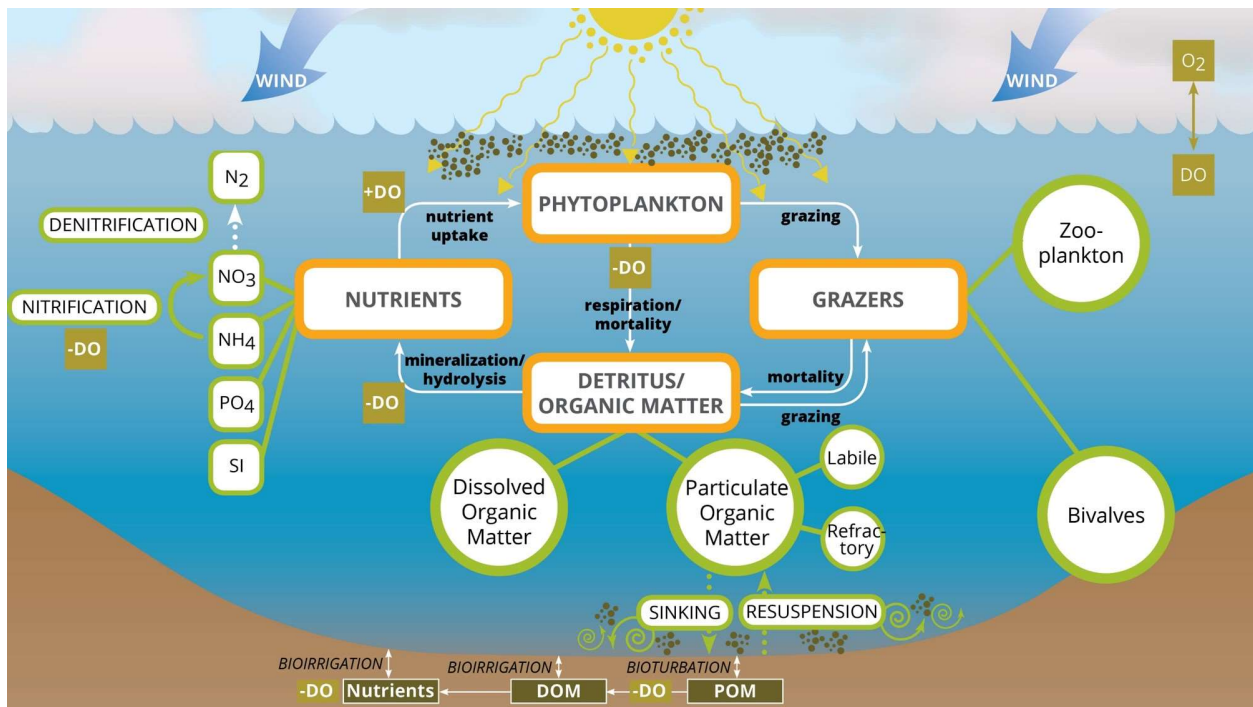


Figure 1 The biogeochemical model structure implemented in DELWAQ

4.1.1 Nutrient cycling

We modeled nitrogen transformation processes including nitrification, denitrification, uptake by phytoplankton, and remineralization by detritus. Nitrification is the oxidation of ammonium (NH_4) to nitrate (NO_3) which is carried out by specialized bacteria and archaea, and this is an autotrophic process (produces energy) requires oxic condition. Denitrification is carried out by facultative anaerobes, in which bioavailable nitrate (NO_3) is converted to nitrogen gas (N_2) through a multistep process and released to the atmosphere, and this is a heterotrophic process that requires anoxic conditions. In the water column, both nitrification and denitrification contribute to nitrogen transformations, but denitrification is generally expected to occur mainly in the surficial layers of bed sediments due to the generally oxygen-rich condition in the water column for our system; however, some denitrification may also occur within anoxic microzones associated with suspended particulate matter in the water column.

Nitrification rate is modeled as a first-order rate depending on ammonia concentration, dissolved oxygen concentration and temperature, whereas sediment denitrification rate is only dependent on temperature and local depth (*SFEI*, 2018). The first order denitrification rate can also be replaced with a complex sediment diagenesis model, which we made possible as described in detail in section 4.1.4. Although the current DELWAQ model has the capability to model the sediment diagenesis process, it is not routinely turned on during the model tuning phase due to the limited data available to calibrate the process, the long computational time it incurs, and the small difference it makes in the modeling results.

4.1.2 Phytoplankton dynamics

The rate of change in phytoplankton biomass is determined by transport, growth rate, mortality rate, and respiration rate of phytoplankton. Phytoplankton growth (or the synthesis process) is modeled as a function of nutrient concentrations, light availability, and temperature. Both nutrient and light availability can limit phytoplankton growth. The mortality rate includes death via natural mortality and grazing by primary consumers, including zooplankton and clams. Detritus or particulate organic matter is released from algal predation, algal and zooplankton metabolism (death, maintenance, and faeces). The detritus both within the water column and in the sediment surface can be food sources for zooplankton, although zooplankton in the Delta tend to preferentially graze on phytoplankton and is mainly food-limited by phytoplankton in the system (*Orsi and Mecum*, 1986; *Sobczak et al.*, 2005). The non-living organic matter is comprised of DOM (dissolved organic matter, C, N, P or S) and POM (particulate organic matter). POM will first be converted to DOM through hydrolysis before it can be mineralized. POM can also sink to the bottom and be grazed by bivalves or go through diagenesis in the sediment layers and return to the water column as DOM or DIM (dissolved inorganic matter, such as DIN). The sinking and resuspension of POM is governed by bottom shear stress, which is determined by bottom roughness and a combination of benthic unidirectional flow and wave-driven oscillatory flow. Both mineralization and diagenesis are a function of temperature and proportional to organic matter concentrations.

4.1.3 The Dynamic Energy Budget (DEB) Model for Clams

Based on the first principles of thermodynamics, the Dynamic Energy Budget model developed by *Kooijman* (2000) describes physiological processes individual organism or communities experience during their life cycles. Specifically, these processes include food ingestion, defecation, energy assimilation, storage or reserve dynamics, utilization, growth, maintenance, maturing, reproduction, and spawning (*Troost*, 2009). A simplified diagram illustrating key processes and model variables for the DEB model is presented in Figure 2.

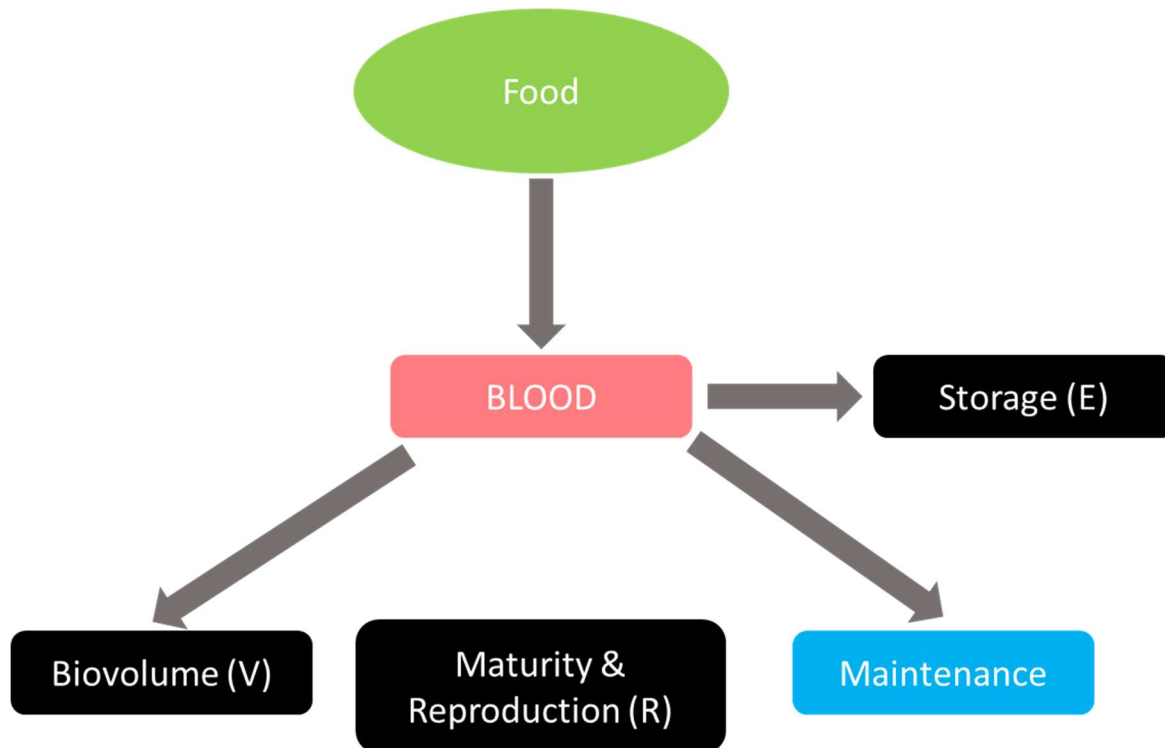


Figure 2 A schematic diagram of the DEB model illustrating how energy generated from food intake is distributed among different compartments of a living organism. The compartments in the black boxes (E, V, and R) are model variables for the DEB model.

We chose to apply a food-dependent dynamic grazing model rather than imposing predefined benthic grazing rates for the following reasons:

- The spatial coverage of the observed clam data for WY2011 is very limited. Using a dynamic model is the best way to minimize errors associated with spatially interpolating clam biomass from a limited number of observational sites, since the modeled clam

biomass will automatically adjust to local food availability and hopefully approach more realistic spatial distribution during the simulation.

- There could be large errors associated with the observed clam biomass. Clam biomass measured at one location may not be representative for the local community.
- Clams themselves can be nutrient sinks/sources.

Compared to a simple first-order grazing rate model, DEB model can more realistically describe the growth or mortality curves of the grazers for the following reasons:

- The DEB model includes an energy reserve term: when food is available, energy is stored in the reserve, which can be used to sustain the metabolism and even growth of clams when food becomes scarce, so the organism can survive longer period of starvation.
- The DEB model has a unique model structure, where the energy assimilation rate (from food) scales linearly with the surface area to volume (and thus biomass) ratio, which decreases as the organism gets bigger. Newly settled clams can grow much faster than older established clams. When an organism reaches its maximum size, energy intake exactly equals maintenance cost and the organism stops growing. This model structure imposes additional constraints on clam growth rate and the percentage of food can be used to support growth during the entire life cycle of clams, so we would not accidentally apply an unrealistic growth rate for the purpose of matching with the observational data.

The DEB model can be run in three modes in DELWAQ: isomorph, V1-morph, and mixed approach. Isomorph is used to model an individual organism or a cohort of organisms at similar life stage, and the size of the bivalves responds to food availability. V1-morph is used to model a community of organisms with different sizes; the community-averaged size of the organisms does not change over time but the density or biomass of the community changes with food availability. A mixed approach models a baseline stable community using V1-morph and known seasonal recruitment of newly settled clams using isomorph. The mixed approach is the most realistic mode for the DEB model, however it is more complex in model structure and requires more observational data (such as recruitment) to set up. In this study, we chose to apply the V1-morph mode to assess if this simplified approach is good enough in capturing the observed clam grazing dynamics in the system.

4.1.4 The Sediment Diagenesis Model

Sediment is composed of inorganic matter, detritus (POM), and algae. At this stage, only detritus is modeled in the sediment model. POM in the sediment is divided into labile (DetX) and refractory (OOX) substances. When POM in the water column sinks to the bottom, it becomes DetX. The sediment diagenesis model includes two layers of sediment: S1 and S2. S1 can be partially enriched with DO (aerobic), but S2 is depleted of DO (anaerobic). We assumed that the sediment had fixed porosities and fixed layer thicknesses, so all advection processes related to flow through the sediment-water interface (i.e., seepage) that affect the benthic geometry and porosity were turned off. One reason we decided to make these assumptions was that we had very little knowledge of parameters needed to model the impact of suspended sediment on the morphology of the sediment layers. However, what we were trying to model were the concentrations of substances in the sediment (organic matter composition) and their exchanges with the water column. Dispersion of dissolved substances (bio-irrigation) causes transport fluxes of dissolved matters across the sediment-water interface. These fluxes include the so-called return fluxes of nutrients to the water column and the sediment oxygen consumption flux. We also turned on bioturbation to represent dispersion of particulate matters between the sediment layers and water column.

4.2 Attribute-dependent model aggregation

The motivation for developing an aggregated model is to significantly reduce the run time required by the biogeochemical model. DELWAQ is coupled with the hydrodynamic models offline. The offline coupling feature allows DELWAQ to be driven by velocity and eddy viscosity fields supplied by other hydrodynamic models, including both Deltares models and non-Deltares models, and saves computational time because hydrodynamic runs do not need to be during the model tuning stage for the water quality model. However, parallel computing is not enabled for DELWAQ, so the model runtime can be long when the number of variables is large. When the complete set of biogeochemical processes is included in the current project, the estimated runtime for one water year can range from 14 to 30 days, which makes model tuning extremely slow. Developing a tool that automatically lower the grid resolution to significantly reduce the runtime is a common goal for SFEI and DELWAQ developers. A desirable algorithm for model aggregation should 1) preserve as much as possible the spatial variance of variables modeled by the full resolution grid; 2) be automatic; 3) prevent aggregation across control structures, such as

levees. We chose to use the spatially constrained multivariate clustering tool provided by ArcGIS pro Mapping Clusters Toolset. The attributes we included were water depth, NO₃, and NH₄. At this stage, we only included representative snapshots of NO₃ and NH₄ but it is possible to include the entire time series of these variables. The clustering algorithm by ArcGIS pro produced polygons with holes and a simple python algorithm was developed to separate those polygons into a minimum number of polygons without holes. The python scripts for both model aggregation and post processing can be found in github repository: <https://github.com/ZhenlinZh/delwaqAggregation.git> and the aggregated grid generated is shown in Figure 3.

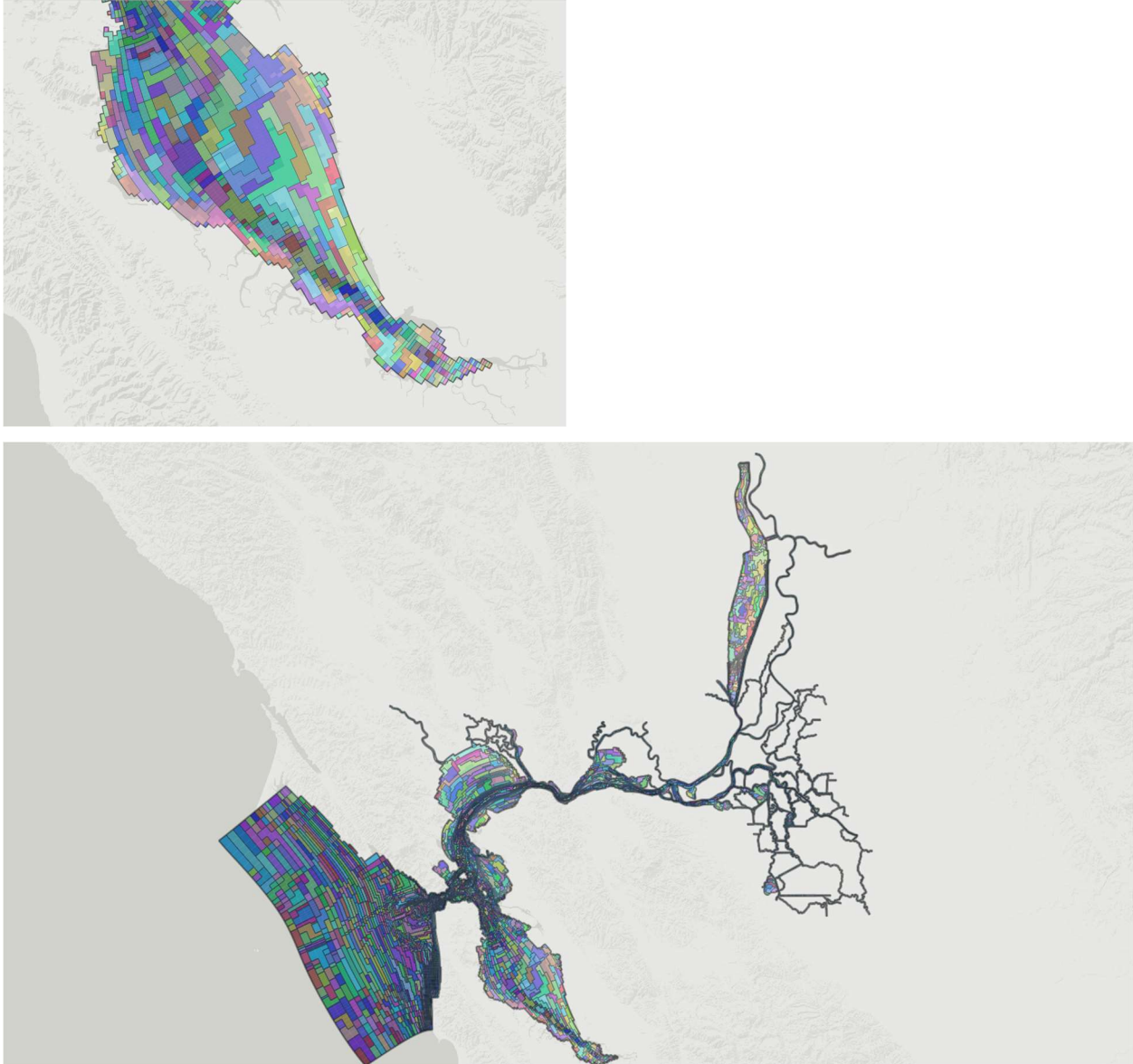


Figure 3 The aggregated grid. Each distinctly colored polygon represents a different cluster of grid cells for the aggregated grid.

The effectiveness of the aggregated model to capture the spatial variability of NO_3 and NH_4 was tested by running DELWAQ with the aggregated grid. The modeled results show that at least within the Delta-Suisun region, the differences between the aggregated model and the full resolution model are small and localized (Figure 4).

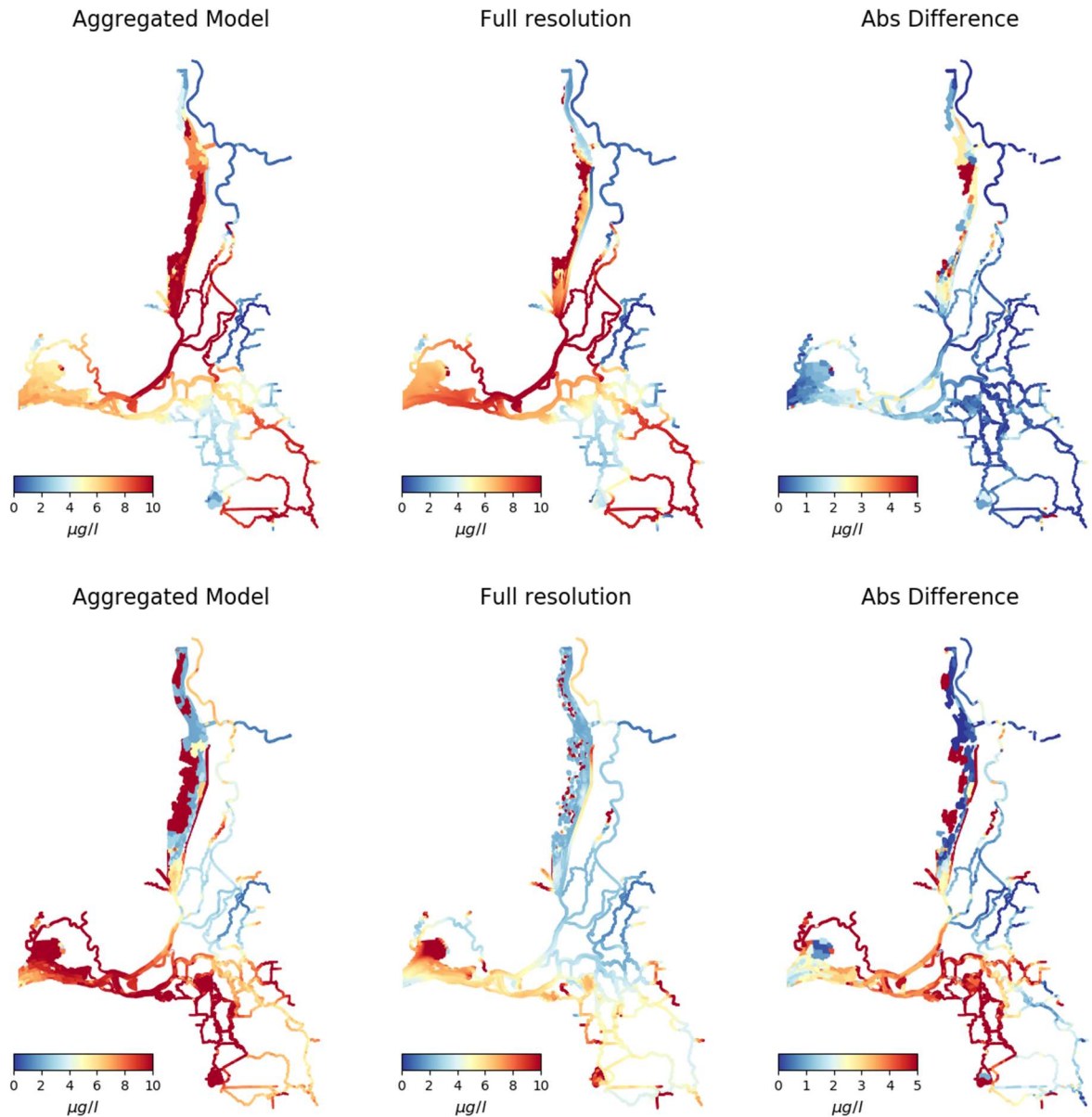


Figure 4 A comparison of modeled NH4 (top) and NO3 (bottom) between the aggregated model (left) and full resolution model (middle), and the difference between the two (right).

4.3 Tuning the Dynamic Energy Budget (DEB) model for benthic grazers

The DEB model was applied to both *Portacorbicula* and *Corbicula* for the Delta-Suisun system. To come up with an initial set of parameters for the model, we first translated a zero-dimensional (0D) DEB model from the DELWAQ source code (in FORTRAN) to PYTHON; we then gathered the community-averaged condition from the measurements for both clams for WY2011 (see Table

1); thirdly, we fed the clams with an ambient chlorophyll-a level of 3 $\mu\text{g/l}$ and tuned the 0D DEB model until the modeled biomass reached steady-state. At least by examining the observational data, an ambient chlorophyll-a of 3 $\mu\text{g/l}$ seems to be the cut-off value, above which, clam biomass increases and below which, it declines. The major tunable parameters are reference length, mortality rate, ingestion efficiency, and half-saturation; all the other parameters should not be changed unless lab measurement for the clams becomes available. To tune the 0D DEB model, we need to satisfy: 1) the clam grazing rate at steady state needs to match with the magnitude of the grazing rate estimated from the measured bivalve biomass; 2) the pumping rate of corbicula is about 4 times that of *Potamocorbula*. An initial set of parameters that satisfies the above objectives and constraints are listed in Table 2.

Table 1 The spatially and temporally averaged condition for both bivalves during the simulation period (WY2011).

| Bivalves | Biomass in AFDW (g/m ²) | Grazing rate in per day | Grazing rate in m/day | Density (# per m ²) | Mean length (cm) | Adult length (cm) | Filtration rate (L water per 10 g tissues per day at 20 °C) ² |
|---------------|-------------------------------------|-------------------------|-----------------------|---------------------------------|------------------|-------------------|--|
| Corbicula | 13 | 0.2 | 0.88 | 900 | 1.79 | 2 to 3 | 1000 |
| Potamocorbula | 7.3 | 0.55 | 2.1 | 2573 | 1.03 | 2.5 | 4000 |

Table 2 The derived rates table from the 0D DEB model satisfying the objective and constraints for model tuning.

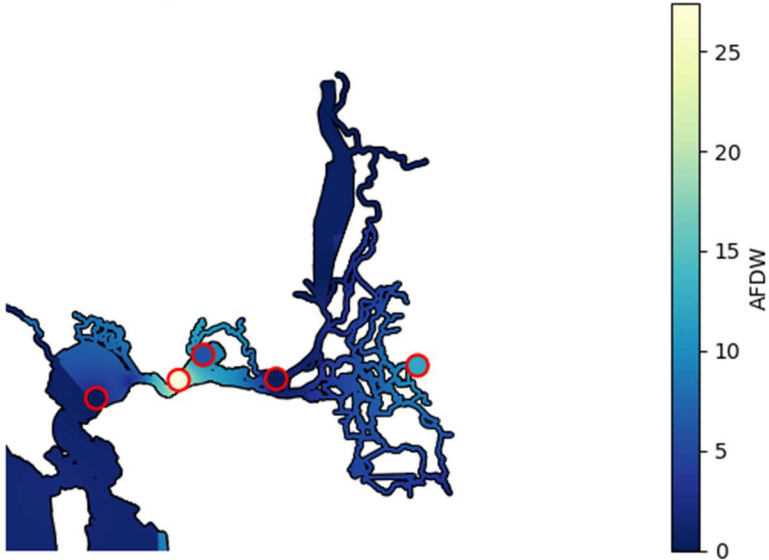
| Bivalves | Individual volume (cm ³) | Length (cm) | Maximum ingestion rate (J/cm ² /d) | Basal respiration rate (J/d) | Reference mortality rate (per day) |
|-----------|--------------------------------------|-------------|---|------------------------------|------------------------------------|
| Corbicula | 0.11 | 1.79 | 40 | 4 | 0.00055 |

² From Cole et al. 1992, the filtration rate or pumping rate (l/g/day) for *Potamocorbula* (with multi-size 5.5 to 20.5mm shell length), is defined as $dx \cdot V/B$. dx is phytoplankton loss rate in per day, and V is the volume of water in the flume, and B is bivalve AFDW. If we time filtration rate with chl-a, we will obtain the grazing rate in gChl-a/g AFDW/day). And the filtration rate is sensitive to flow.

| | | | | | |
|---------------|------|------|-----|----|---------|
| Potamocorbula | 0.02 | 1.03 | 128 | 50 | 0.00055 |
|---------------|------|------|-----|----|---------|

The initial condition of bivalve biomass was spatially interpolated from the observed ash-free dry weight (AFDW) biomass values using the inverse distance weighting method and assuming an AFDW:C ratio of 0.4. The spatial maps used as model initial condition are shown in Figure 5.

IDW 2 point p=1 (Potamocorbula) Biomass



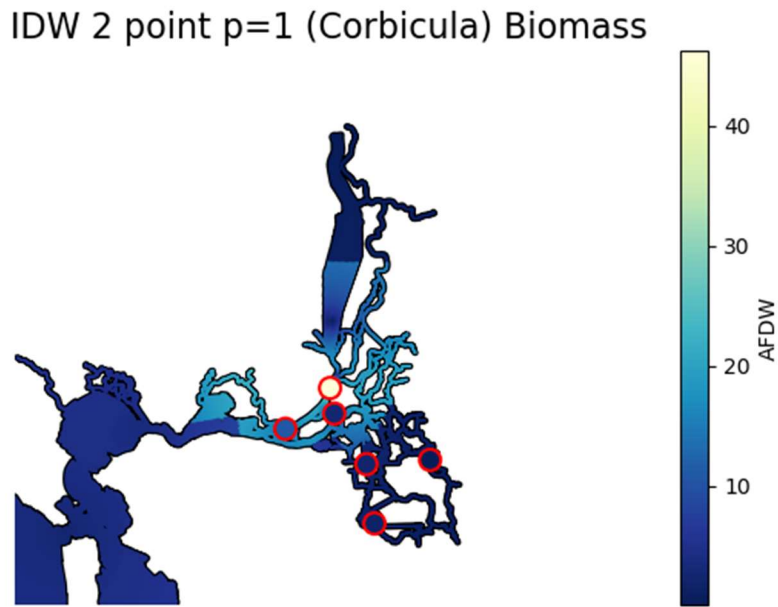


Figure 5 The initial AFDW biomass for Corbicula and Potamocorbu.

5. Results and Discussion

The modeled time series of Chlorophyll-a, NO₃, and NH₄ are presented for various stations in Appendix A. Our model is doing a reasonable job in capturing the spatial and temporal variations in all these variables at most of the stations presented. For chlorophyll-a, only at a few stations and on selected days does our model deviate considerably from the observations (for instance, MD10A in Feb 2011, D41 in March, and P8). These stations have drastically different flow regimes compared to the central Delta and using a spatially homogeneous light extinction coefficient based on the observed turbidity at one central Delta location (at Mallard Island) is mostly likely what contributed to the modeled discrepancy for these stations. The potential error associated with the spatial interpolation of initial clam biomass could be another important source of error. Given all these known issues, our model was still capable of modeling a general non-blooming condition that captured both the spatial and temporal patterns of the observed nutrients and phytoplankton biomass in the Delta.

Although modeling clam biomass is not the focus of the current project, it is still helpful for us to check and make sure that the grazing pressure imposed on phytoplankton was reasonable in our

model. Comparisons between the modeled and observed bivalve biomass for both *Corbicula* and *Potamocorbula* are presented in Appendix B. The modeled results show that our model correctly captured the baseline magnitudes of the biomass and some seasonality. The short-term variations (those peaks in the observed AFDW of clams that start and end within less than 2 months) cannot be captured by the current mode of the DEB model. This may be because:

- 1) Such short-term variations may not be real. The observed clam biomass from the sampling location may not be representative of the spatially averaged biomass for the local community; and the error bar (or variance) associated with the observations is unknown but can potentially be large.
- 2) The occurrence of these peaks could have been associated with the recruitment of newly settled clams, who grew much faster than the community-averaged clams, due to their much smaller size. Because we assumed a V1-morph model with a constant community-averaged organism length, recent recruitment of a large number of newly settled clams cannot be modeled. This may explain some of the short-term variations in the observed biomass, such as at D7 and D28, that we failed to capture.

However, what we hope to improve is the under prediction of clam biomass during the summer of 2011 that was consistently observed at multiple locations (e.g., D4, D24, C9, and D6). To improve the prediction, more food needs to be channeled to supply the growth of the clams during the period. There are potentially two approaches we can try to achieve this:

- 1) Including clam grazing on other unbudgeted food sources: terrestrial allochthonous organic matter and zooplankton. In the most recent model run, we turned on grazing on detritus by clams, which helped deliver more food to the clams and improved the modeled clam biomass. Without grazing on detritus, the model clam biomass will slowly decline and diverge from the reality. This suggests that food sources other than phytoplankton, particularly detritus, are required to maintain the observed growth rate of both clams during WY2011. However, in our model, detritus only originates from recently dead phytoplankton and zooplankton. Allochthonous particulate organic matter from river inflow, irrigation outflow, ponds and floodplains has not been included in the model and may be a cause of the underestimation of clam biomass.
- 2) We need to make sure that vertical mixing is properly modeled by the hydrodynamic model (CASCaDE project). A comparison between the wind fields used by the CASCaDE

project and those measured show that the former was generally lower than the observational values in the Delta (*King, 2019*); wind-induced surface waves are also not included in the current version of the hydrodynamic model. Both will result in less turbulent mixing and lead to less food delivered to the clams.

Using the calibrated biogeochemical model, we performed two hypothetical scenario runs: 1) removing clams and 2) increasing phytoplankton growth rate by 25%. The motivation to perform the first scenario is that it is hypothesized that the introduction of the invasive clam (*Potamocorbula*) caused the shift from high bloom to low phytoplankton biomass conditions for the system in 1986. The second scenario represents the condition where either solar radiation increases or turbidity decreases (or some combination of the two) by 25%. Given that the turbidity in the system has declined by 50% from the 1980s to 2010 (*Cloern and Jassby, 2012*), a further decrease of 25% could be within the possible range of scenarios for the next two decades. The model results at D7 show that, when clams are removed, phytoplankton biomass reaches 30 $\mu\text{g/l}$ and the biggest differences between the runs with and without clams occur during the warmer months of the year (from May to Oct; see Figure 6). These model results agree very well with historical observations of the change in phytoplankton biomass and in the months where the largest difference at this station between pre- and post-bloom conditions were observed (Figure 3 and 6 in *Cloern, 2018*). This finding suggests that our model correctly captured the dynamics of clam grazing for the system. It is also interesting to notice that, for the no-clam run, DIN was substantially lower than the scenario with the clams during the phytoplankton bloom event and the phytoplankton growth rate was strongly nutrient limited (shown by nutrient limitation factor, which indicates no nutrient limitation when it is equal to 1 and extreme limitation when it is equal to 0).

The presence of the bivalves indeed effectively reduced phytoplankton blooms, particularly during the warmer months of the year. However, can the clams prevent any blooms from happening in the system? The second scenario run with increased growth rate showed that even with the presence of clams, phytoplankton blooms can still occur when other conditions support them. Moreover, extreme nutrient limitations are observed at both a shallow (D7) and a deep (USGS 649) stations during the bloom event (Figure 7).

The fact that nutrient limitations are observed either when clams are removed or when phytoplankton growth rate is increased at multiple locations emphasizes that nutrient source control (such as the Sac Regional upgrade) is likely to be effective in reducing phytoplankton biomass and productivity for the ecosystem.

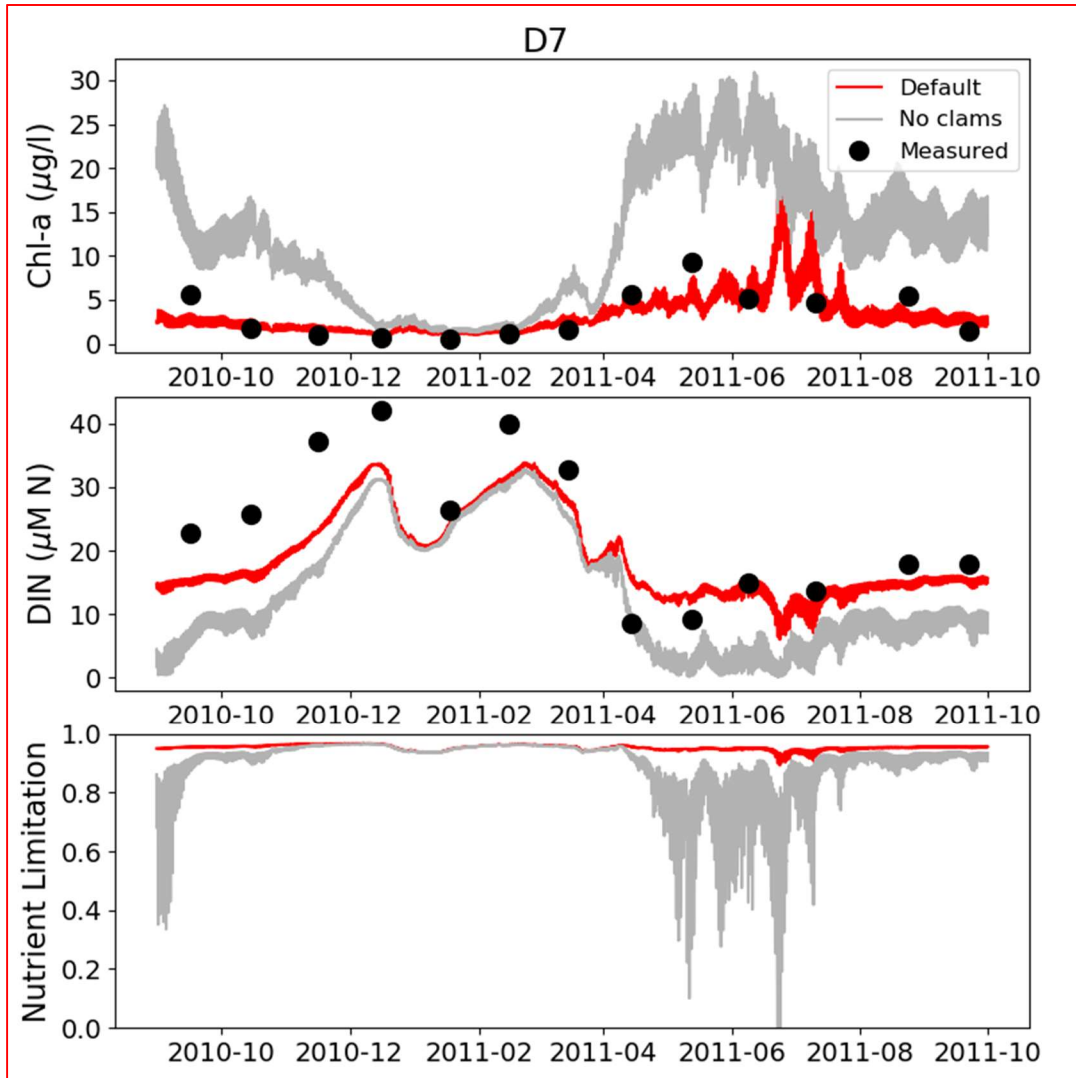


Figure 6 Comparisons of model results between scenarios with clams (default) and without clams (no clams).

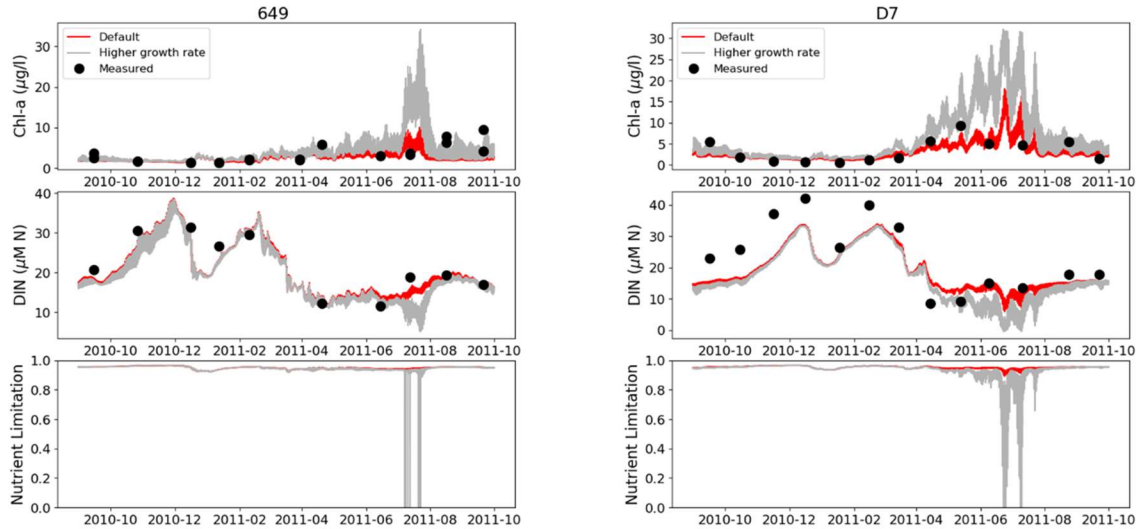


Figure 7 Comparisons of model results between the default run and the scenario run with increased growth rate for a deep (USGS 649 on the left) and a shallow location (D7 on the right).

6. Future Work:

Further improvement of the model requires implementing better spatial variations of environmental forcing conditions, including light extinction coefficient and clam initial biomass. The robustness of the model will also be tested for a different water year (WY2016), where phytoplankton bloom events were observed. The discrepancy between the modeled and observed clam biomass may need additional parameter tuning. The demonstrated importance of turbulent mixing in delivering phytoplankton to the benthic grazers requires rigorous model validation for vertical mixing processes by the hydrodynamic model and accurate atmospheric forcing data that drives it. Further improving the model may also require collecting additional data to 1) generate higher spatial resolution input for clam biomass for regions of particular interest; 2) evaluate the influence of terrestrial allochthonous particulate organic matter; 3) validate hydrodynamic model with observed vertical profiles of flow, temperature and salinity.

References

- Cloern, J. E. (2018). Patterns, pace, and processes of water-quality variability in a long-studied estuary. *Limnology and Oceanography*. <https://doi.org/10.1002/lno.10958>
- Cloern, J. E., & Jassby, A. D. (2012). Drivers of change in estuarine-coastal ecosystems: Discoveries from four decades of study in San Francisco Bay. *Reviews of Geophysics*, 50(4). <https://doi.org/10.1029/2012RG000397>
- Crauder, J., Thompson, J., Parchaso, R., Anduaga, R., Pearson, S., Gehrts, K., et al. (2016). *Bivalve Effects on the Food Web Supporting Delta Smelt—A Long-Term Study of Bivalve Recruitment, Biomass, and Grazing Rate Patterns with Varying Freshwater Outflow* (Open-File Report No. 2016–1005). U.S. Department of the Interior; U.S. Geological Survey.
- Jassby, A. (2008). Phytoplankton in the Upper San Francisco Estuary: Recent Biomass Trends, Their Causes, and Their Trophic Significance. *San Francisco Estuary and Watershed Science*, 6(1). Retrieved from <https://escholarship.org/uc/item/71h077r1>
- Kimmerer, W., Gartside, E., & Orsi, J. (1994). Predation by an introduced clam as the likely cause of substantial declines in zooplankton of San Francisco Bay. *Marine Ecology Progress Series*, 113, 81–93. <https://doi.org/10.3354/meps113081>
- King, A. (2019). *Wind Over San Francisco Bay and the Sacramento-San Joaquin River Delta: Forcing for Hydrodynamic Models*. San Francisco Estuary Institute.
- Kooijman, S. A. L. M. (2000). *Dynamic Energy and Mass Budgets in Biological Systems* (2nd ed.). Cambridge University Press.
- NPDES Permit. (2010). *ORDER R5-2016-0020. NPDES NO. CA0077682. Waste Discharge Requirements for the Sacramento Regional County Sanitation District Sacramento Regional*

Wastewater Treatment Plant Sacramento County. California Regional Water Quality Control Board, Central Valley Region.

- Orsi, J. J., & Mecum, W. L. (1986). Zooplankton Distribution and Abundance in the Sacramento-San Joaquin Delta in Relation to Certain Environmental Factors. *Estuaries*, 9(4), 326. <https://doi.org/10.2307/1351412>
- Schoellhamer, D. H. (2011). Sudden Clearing of Estuarine Waters upon Crossing the Threshold from Transport to Supply Regulation of Sediment Transport as an Erodible Sediment Pool is Depleted: San Francisco Bay, 1999. *Estuaries and Coasts*, 34(5), 885–899. <https://doi.org/10.1007/s12237-011-9382-x>
- SFEI (2014). Senn, D., & Novick, E. *Scientific Foundation for the San Francisco Bay Nutrient Management Strategy* (Draft FINAL). San Francisco Estuary Institute. Retrieved from http://sfbaynutrients.sfei.org/sites/default/files/SFBNutrientConceptualModel_Draft_Final_Oct2014.pdf
- SFEI (2015). Novick, E., Holleman, R., Jabusch, T., Sun, J., Trowbridge, P., Senn, D., et al. *Characterizing and quantifying nutrient sources, sinks and transformations in the Delta: synthesis, modeling, and recommendations for monitoring*. San Francisco Estuary Institute. Retrieved from <http://www.sfei.org/documents/characterizing-and-quantifying-nutrient-sources-sinks-and-transformations-delta-synthesis>
- SFEI (2018). Zhang, Z., Senn, D., Holleman, R., & Nuss, E. (2018). *Annual Progress Report for Delta-Suisun Bay Biogeochemical Modeling Project* (Progress report). Richmond, CA: San Francisco Estuary Institute. Retrieved from http://sfbaynutrients.sfei.org/sites/default/files/2018_nms_fy2018_annual_report.pdf

Sobczak, W. V., Cloern, J. E., Jassby, A. D., Cole, B. E., Schraga, T. S., & Arnsberg, A. (2005).

Detritus fuels ecosystem metabolism but not metazoan food webs in San Francisco

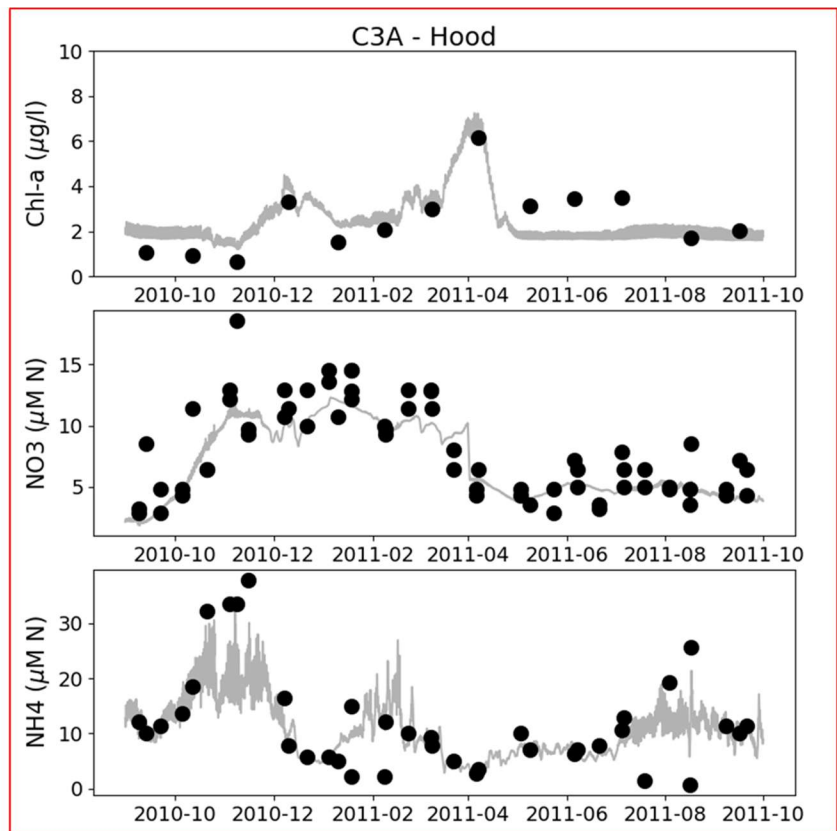
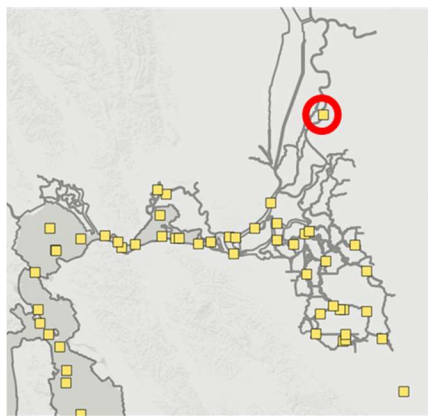
estuary's freshwater delta. *Estuaries*, 28(1), 124–137. <https://doi.org/10.1007/BF02732759>

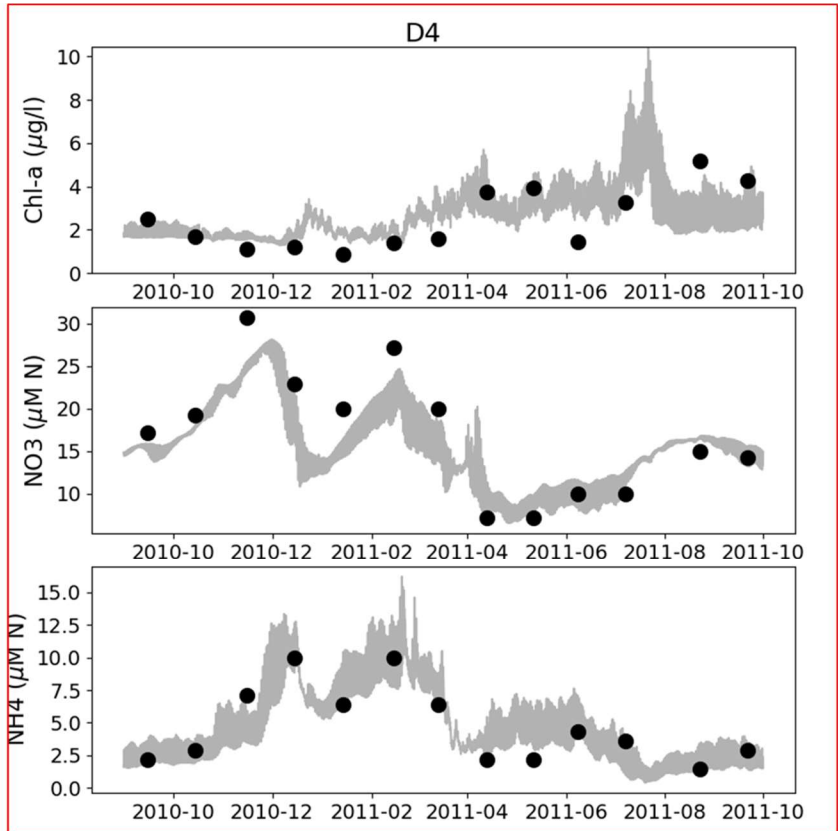
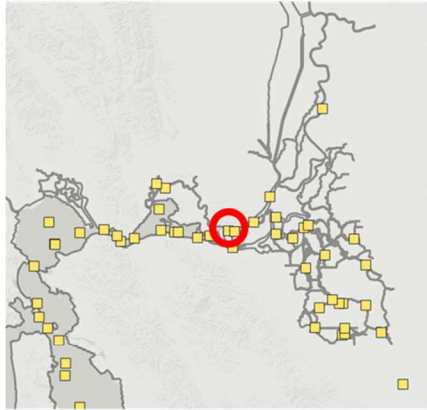
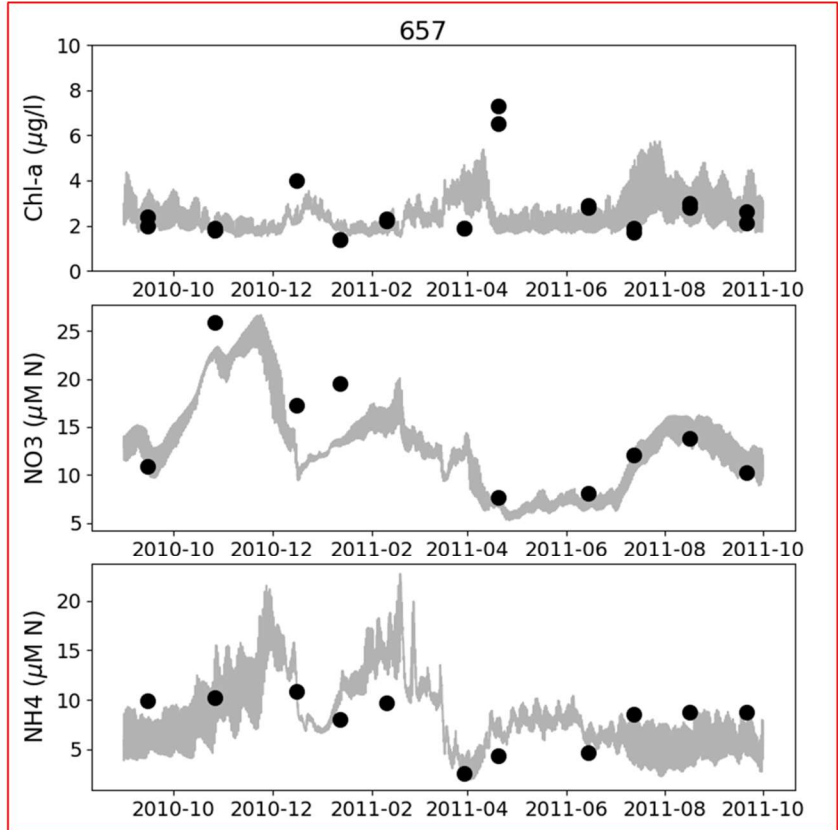
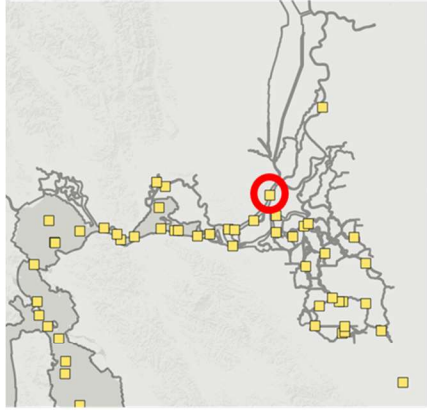
Troost, T. (2009). *Deltakennis Modeling Carry Capacity*. Deltares. Retrieved from

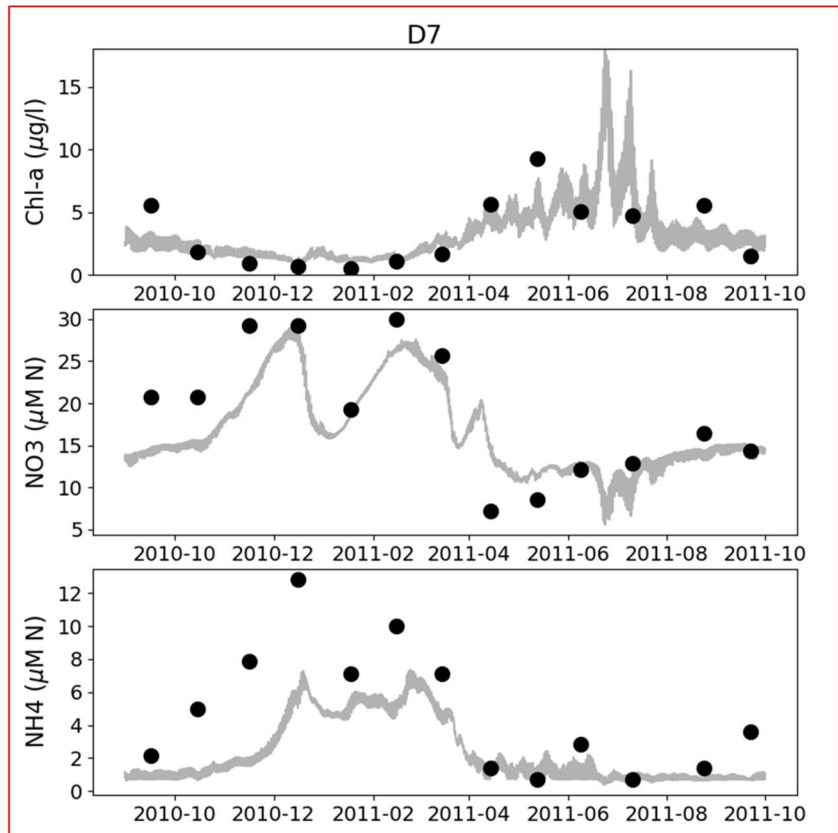
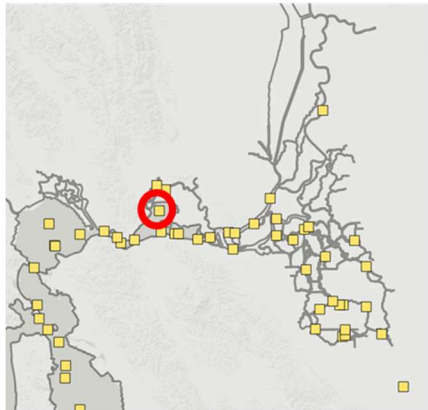
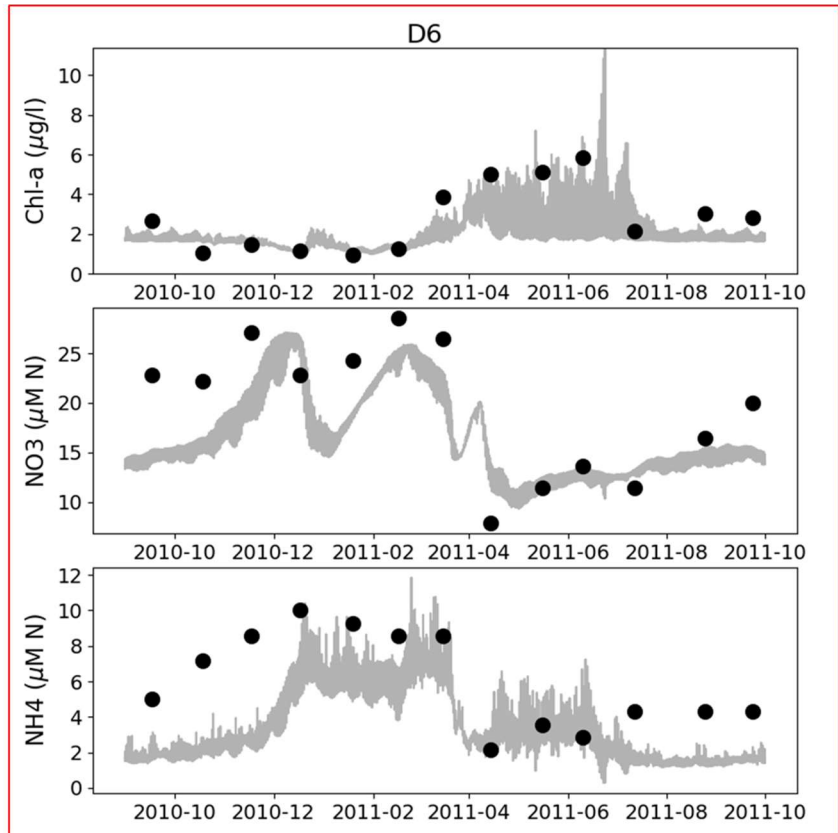
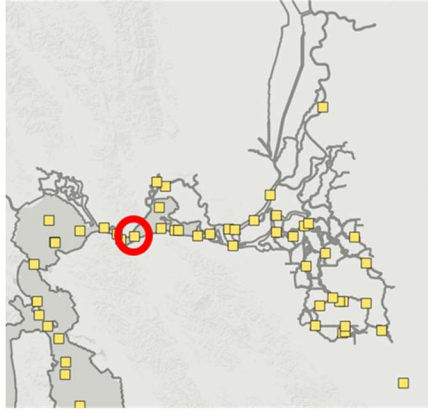
http://publications.deltares.nl/1200314_001.pdf

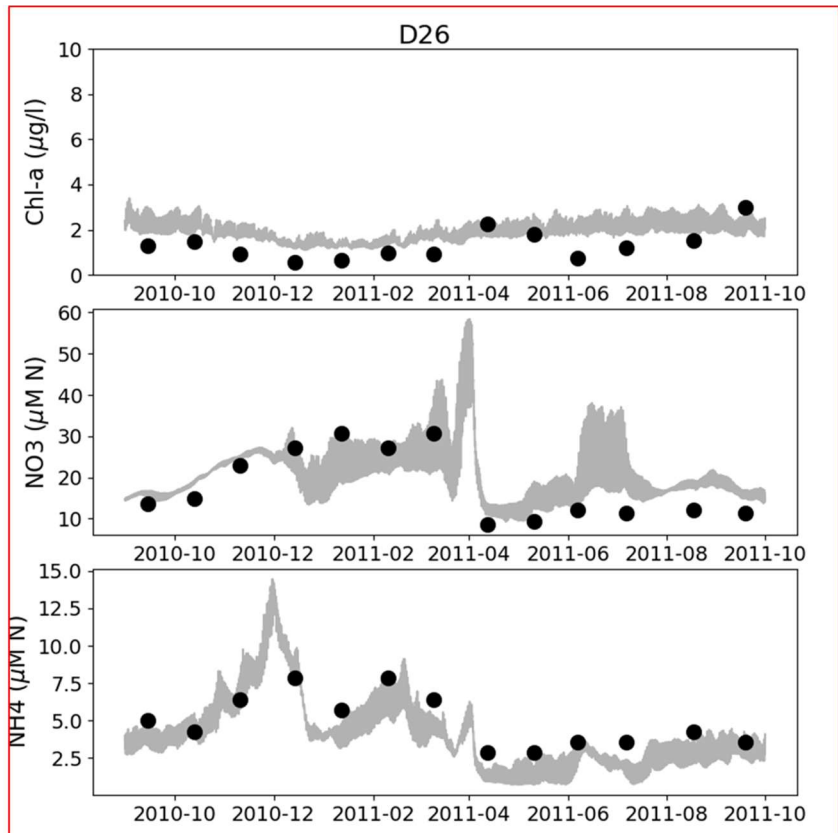
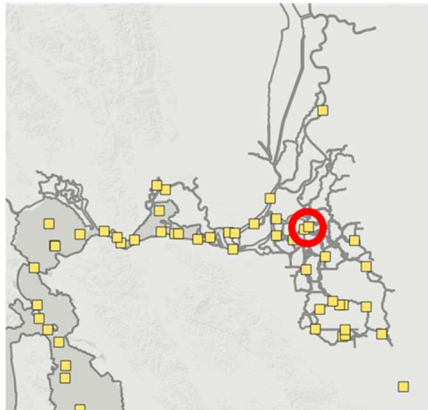
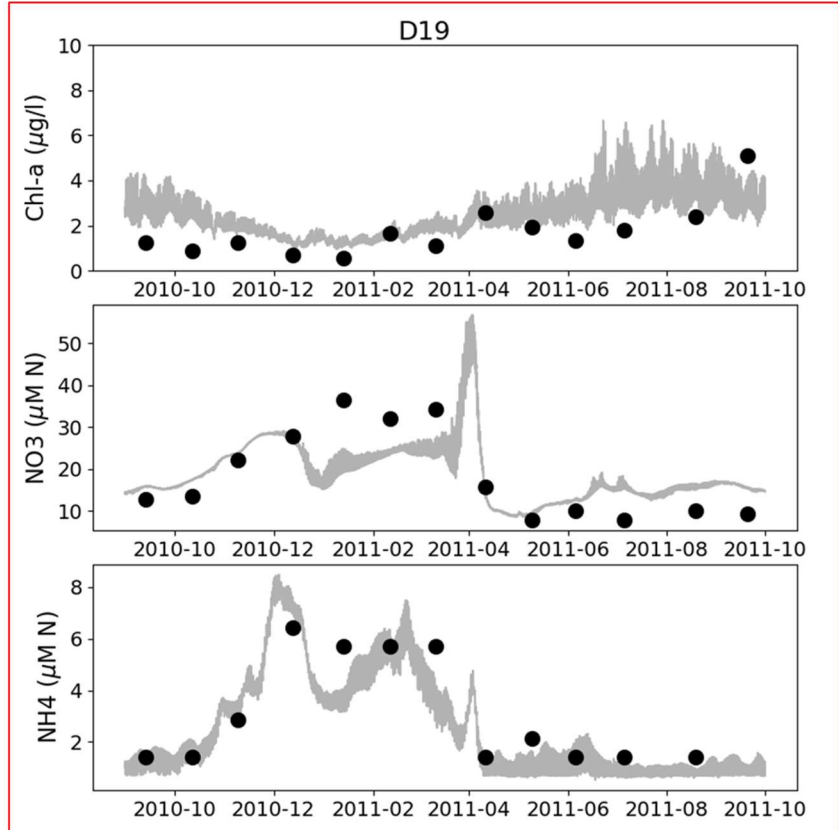
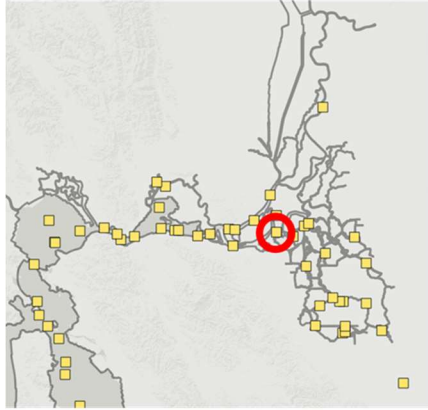
Appendix A The comparison between modeled vs. observed chlorophyll-a, NO₃ and NH₄ at multiple locations across the Delta and Suisun bay.

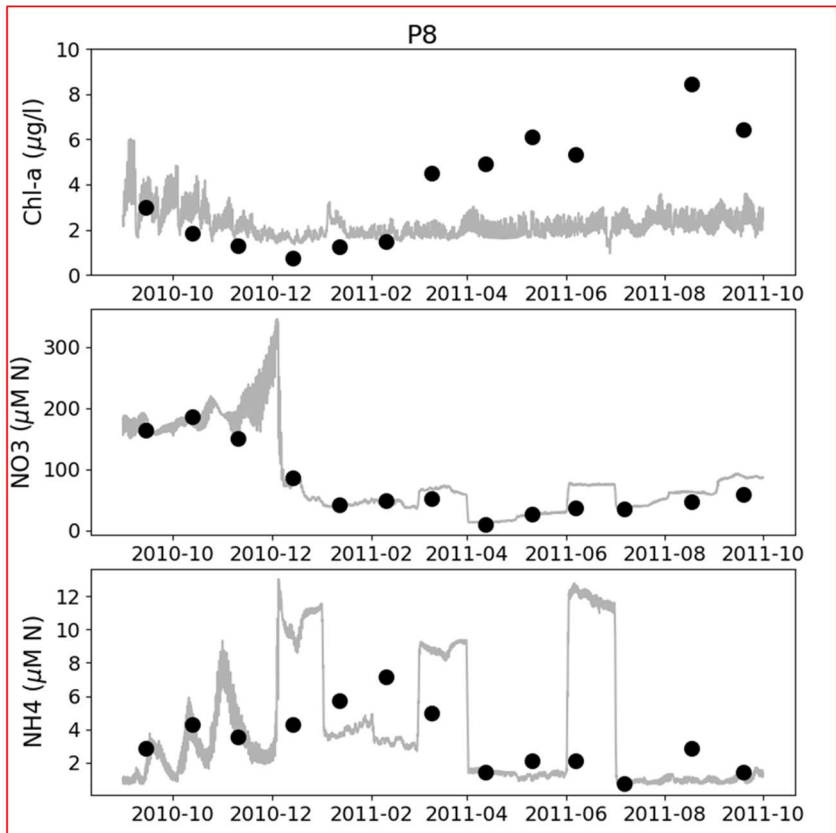
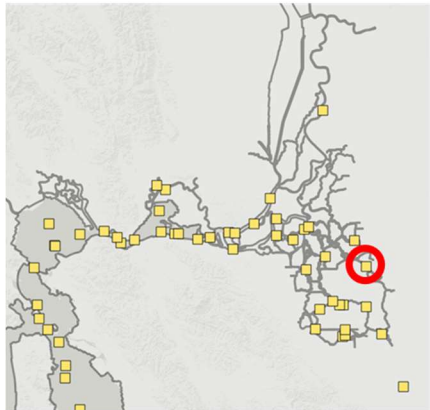
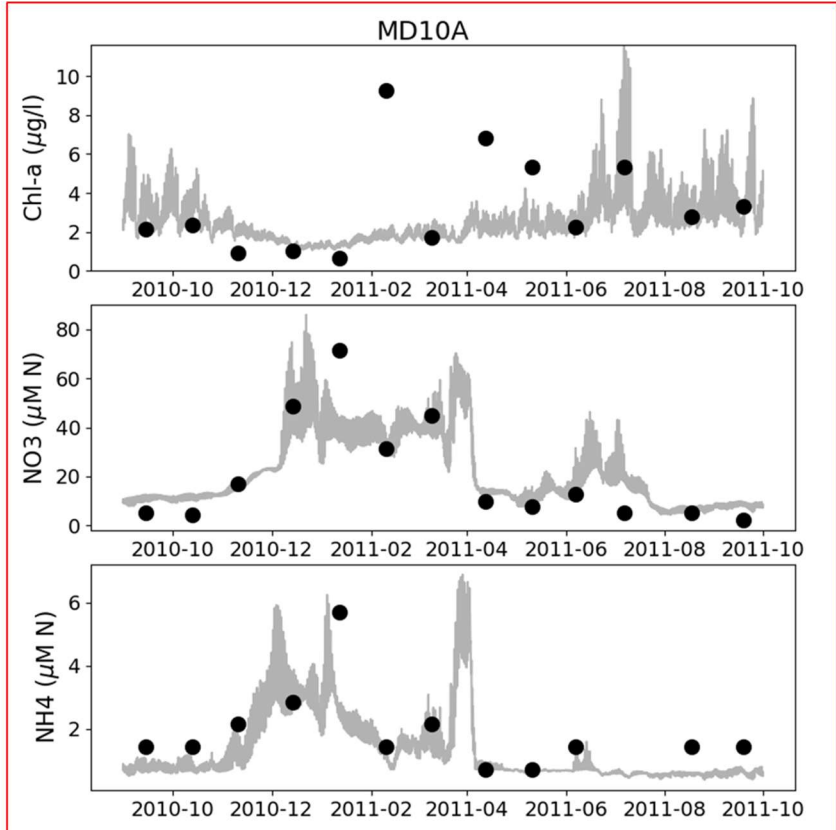
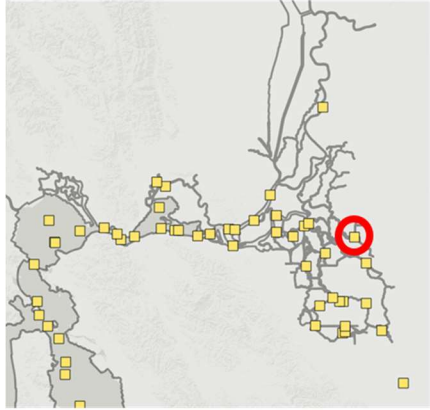
In the following figures, the dots represent measurements and gray lines represents the modeling results.

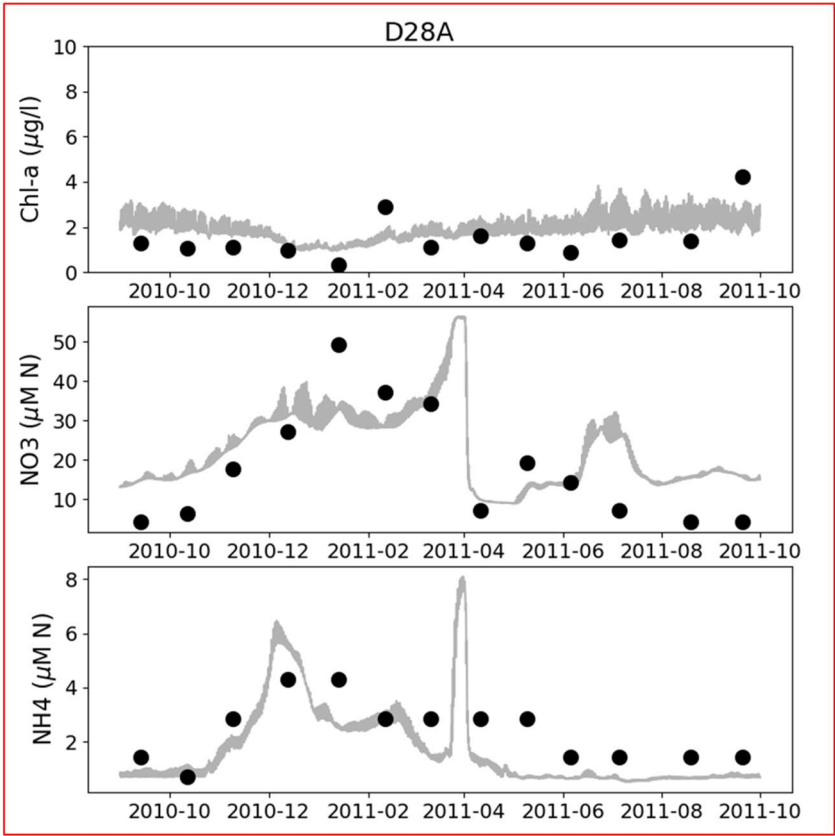
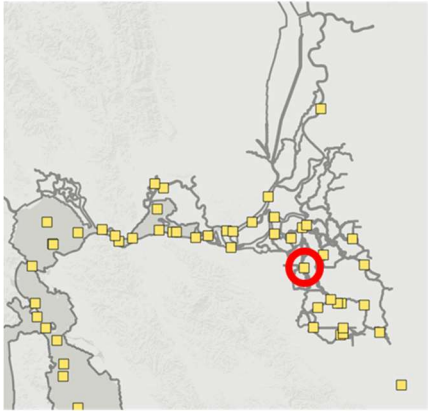




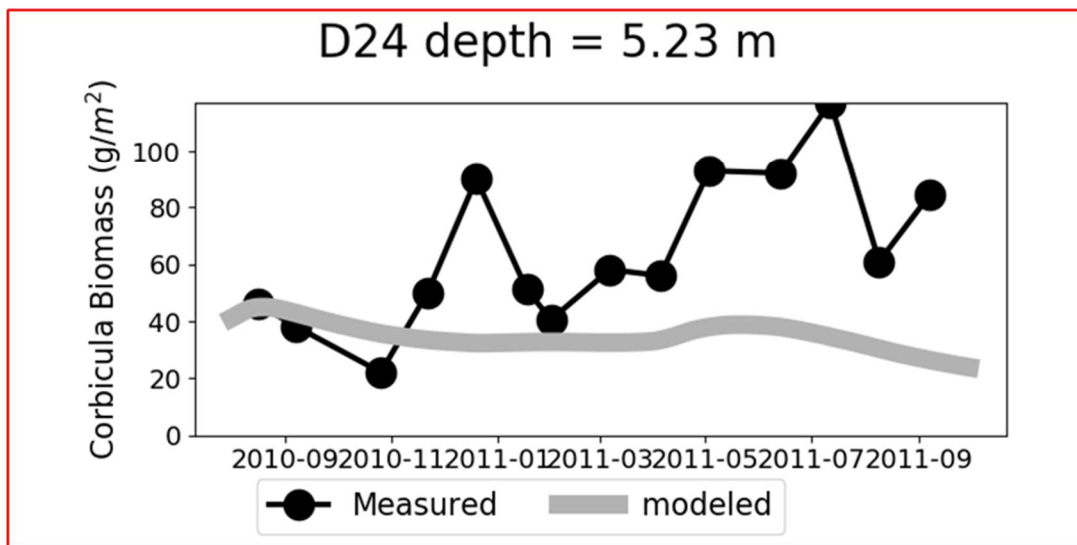
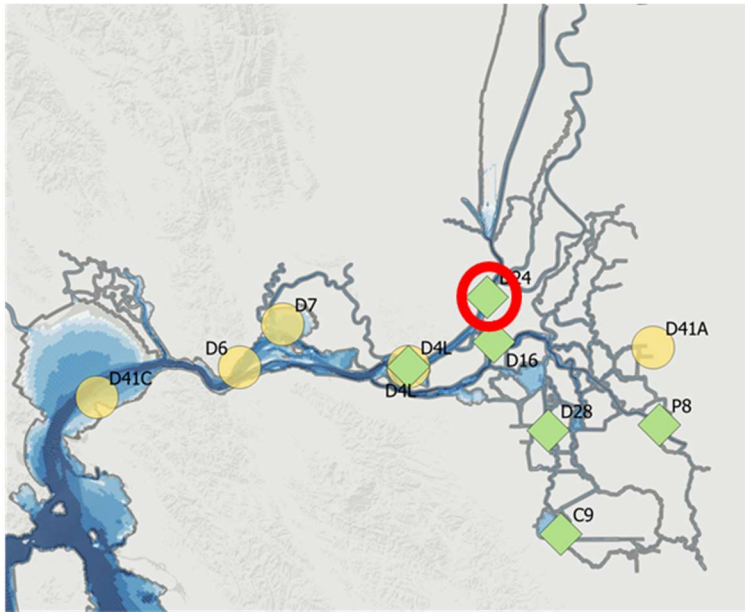


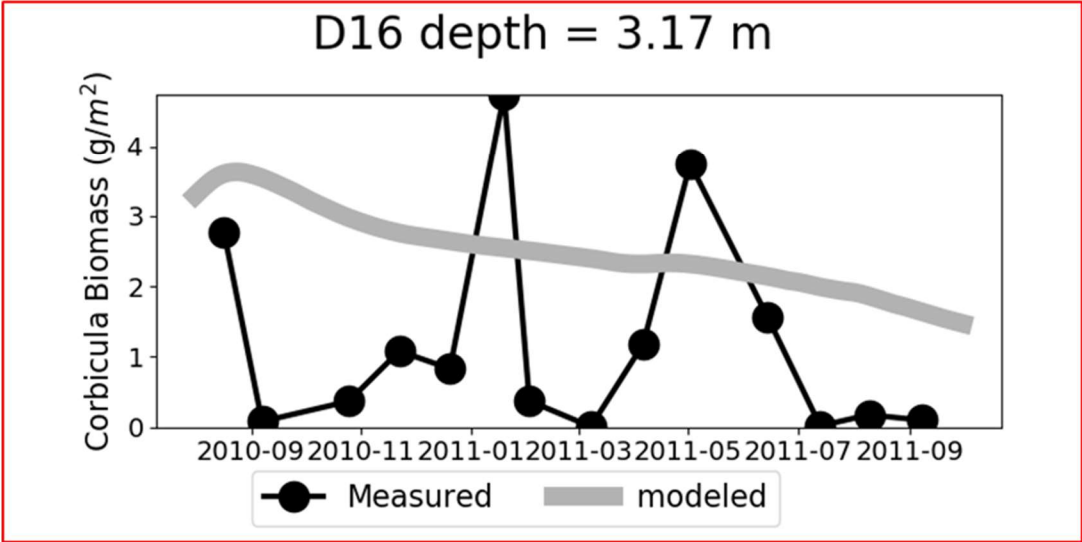
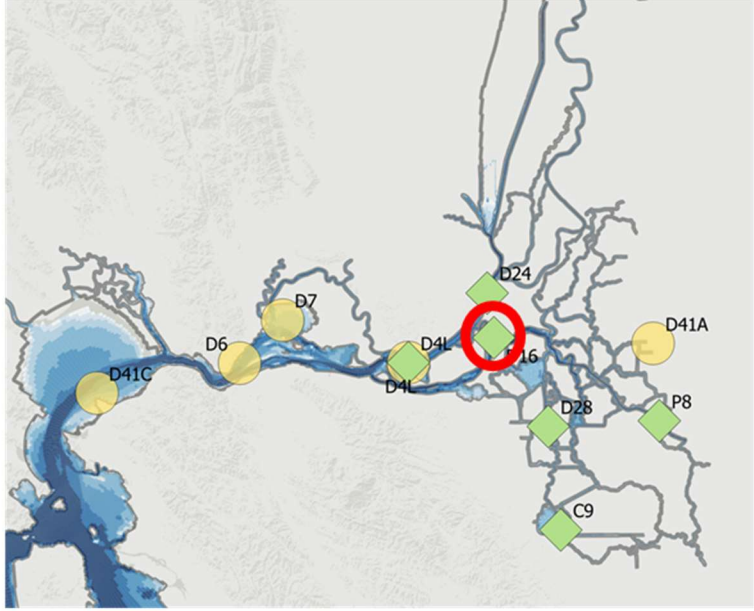


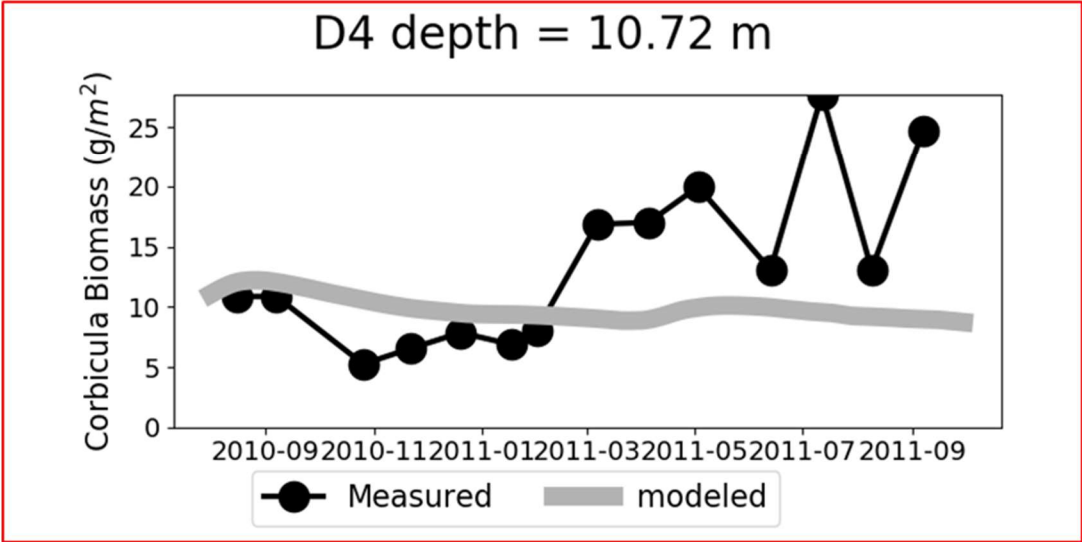
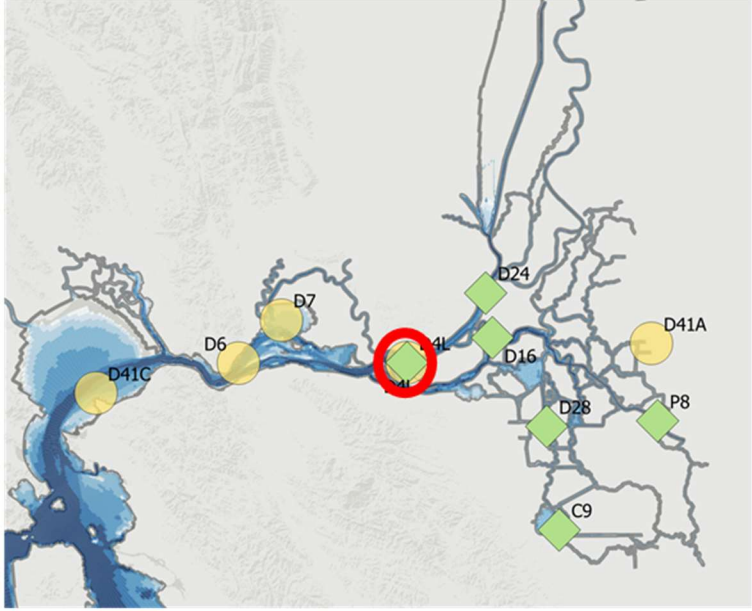


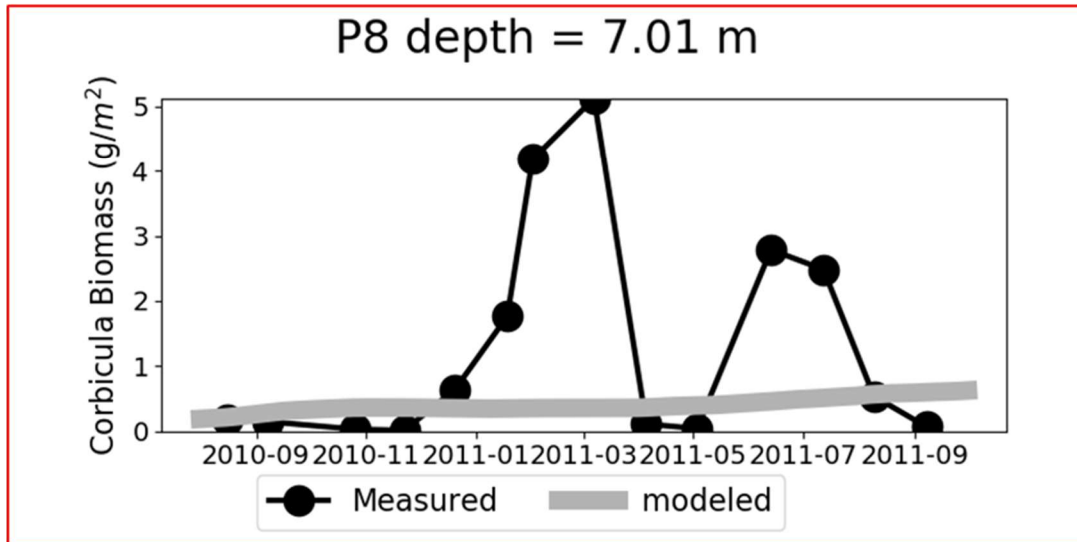
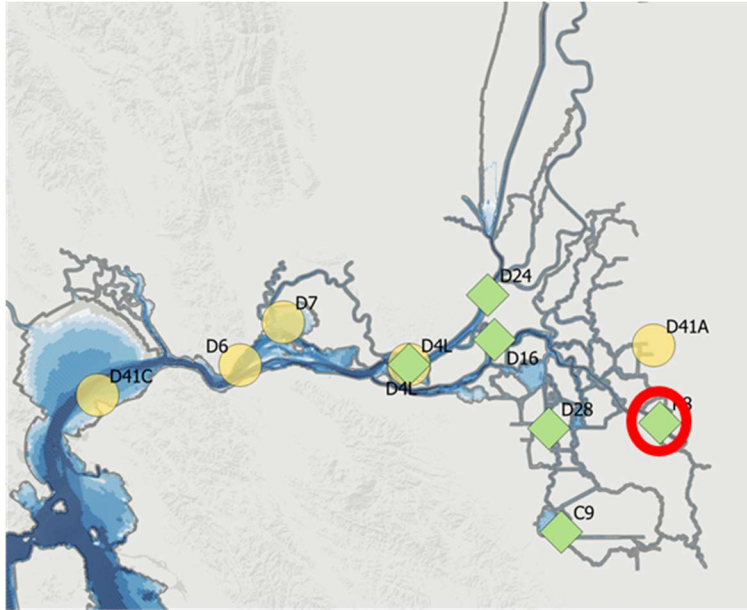


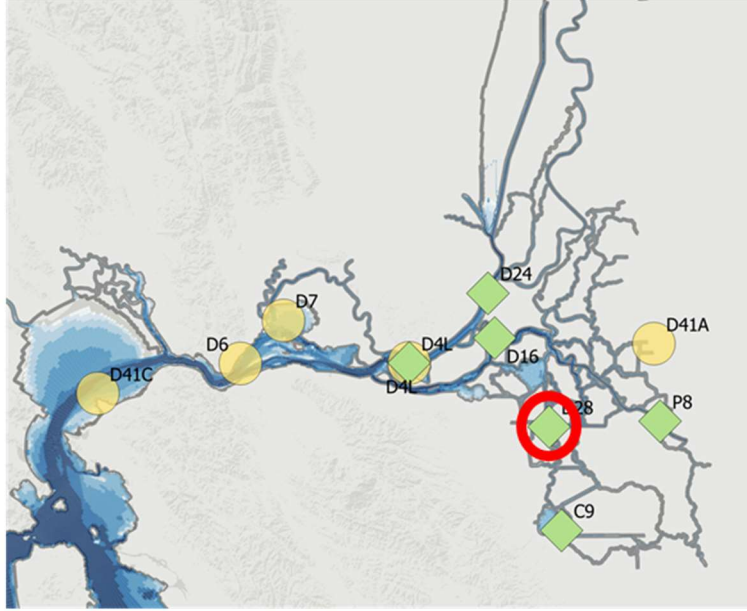
Appendix B Comparisons between modeled clam grazing rate and calculated maximum grazing rate for multiple locations across the Delta and Suisun Bay.











D28 depth = 8.90 m

